A NEW ASSESSMENT OF THE LOFT-WYLE BLOWDOWN TEST WSB03R USING RELAP5-3D

B. R. BANDINI
D. L. AUMILLER
E. T. TOMLINSON

DE-AC11-98PN38206

NOTICE

This report was prepared as an account of work sponsored by the United States Government. Neither the United States, nor the United States Department of Energy, nor any of their employees, nor any of their contractors, subcontractors, or their employees, makes any warranty, express or implied, or assumes any legal liability or responsibility for the accuracy, completeness or usefulness of any information, apparatus, product or process disclosed, or represents that its use would not infringe privately owned rights.

BETTIS ATOMIC POWER LABORATORY WEST MIFFLIN, PENNSYLVANIA 15122-0079

Operated for the U.S. Department of Energy
by Bechtel Bettis, Inc.

A NEW ASSESSMENT OF THE LOFT-WYLE BLOWDOWN TEST WSB03R USING RELAP5-3D

B. R. Bandini
D.L. Aumiller
E.T. Tomlinson

Bechtel Bettis, Inc.
Bettis Atomic Power Laboratory
P.O. Box 79
West Mifflin, PA 15122-0079

Abstract

The RELAP5-3D (version bt03) computer program was used to assess the LOFT-Wyle blowdown test (WSB03R). The primary goal of this new assessment is to represent faithfully the experimental facility and instrumentation using the latest three-dimensional fluid flow modeling capability available in RELAP5-3D. In addition, since RELAP5-3D represents a relatively new and significant upgrade to the capabilities of the RELAP5 series of computer programs, this study serves to add to its growing assessment base.

The LOFT-Wyle Transient Fluid Calibration test facility consisted of an approximately 5.4 m^3 pressure vessel with a flow skirt which created an annulus that acted as a downcomer. An instrumented blowdown loop with an orifice was connected to the downcomer. This facility, built to calibrate the orifices used in several of the LOFT experiments, simulated the LOFT reactor vessel and broken loop cold leg. For the present assessment an existing RELAP5 model developed at INEEL was corrected and upgraded. The model corrections included: 1) employing the proper measured downcomer thickness, 2) positioning the experimental instrumentation in its correct location, and 3) setting the fluid conditions to their measured initial values. Model upgrades included: 1) use of more finely-detailed fluid component nodalization, 2) explicit modeling of the experimental facility beyond the blowdown orifice, 3) addition of heat structure components to represent the heat capacity of structural material, and 4) use of three-dimensional fluid components to model asymmetric portions of the facility.

The new assessment highlights the need to model explicitly the effects of heat storage in structural materials for slowly evolving transients. The assessment also highlights the sensitivity of choked-flow limited calculations to: 1) the model employed, 2) input discharge coefficient values and/or 3) input non-equilibrium values. In addition, the assessment demonstrates that an instability in the calculated liquid fraction at the base of the downcomer obtained using the standard RELAP5-3D Kataoka-Ishii drift-flux correlation can be substantially mitigated through the use of the optional Gardner correlation in the fully one-dimensional model. Finally, the new assessment demonstrates the correct functioning of the three-dimensional fluid components. For this particular transient, three-dimensional modeling does not significantly alter or improve agreement with the experimental data in comparison with an equivalent model consisting entirely of one-dimensional fluid components. This assessment shows that the Vea-Lahey drift-flux correlation in conjunction with the modified LeVeque momentum flux-splitting model is required to dampen liquid fraction oscillations at the vessel/downcomer interface in the 3-D model.

Introduction

Many of the transients of interest to the thermal-hydraulic safety community (Loss of Coolant Accidents) are characterized by fast depressurization due to the loss of liquid inventory. This depressurization causes flashing of the liquid as the pressure falls below the saturation pressure for the fluid temperature. Accurate predictions of the time-dependent fluid inventory loss rate through a choked orifice in the presence of flashing and varying void distribution profiles in various system components are important for thermal-hydraulic safety programs.

In 1979, Wyle Laboratories in Norco, California conducted a series of experiments in the LOFT Transient Fluid Calibration Facility [1] to measure the critical flow rate through LOFT break orifices of varying sizes (nozzles L3-1 and L3-2) during depressurization transients with varying initial conditions. The objectives of these tests were to obtain orifice calibration data at fluid conditions typical of small break loss-of-coolant accidents and to provide a data base for critical flow model development. One of these tests (WSB03R, initiated at 14.7MPa (2148 psia) and 557K (542.9 °F) with a 16 mm (0.6374 in.) break orifice) has become a standard verification problem for the RELAP5 program [2]. The WSB03R assessment is updated herein using the latest version of RELAP5-3D [3]. The result is a model which faithfully represents the full test facility, provides improved accuracy relative to the experimental data, and serves as an addition to the growing assessment base for RELAP5-3D.

Description of the Test

The LOFT-Wyle critical flow experiments were designed to measure transient critical flow rate and fluid conditions (pressure, temperature, and density) upstream of the orifice within the blowdown line during a depressurization transient. Two different orifice sizes (4 mm and 16 mm nominal diameter) were used in the experimental program. This paper will focus on test WSB03R performed with the larger of the two orifices with initial fluid conditions of 14.7MPa and 557K.

A schematic of the LOFT-Wyle Transient Fluid Calibration Facility is shown in Figure 1. The facility hardware consisted of a pressure vessel and a blowdown leg. These components are similiar to the LOFT reactor vessel and broken loop cold leg.

The pressure vessel was made from carbon steel, with a volume of approximately 5.4 m^3 (190 ft^3). The pressure vessel contained a 0.01905 m (0.75 in.) thick carbon steel flow skirt to create an annulus for the LOFT downcomer. The flow skirt extended 0.8382 m (33 in.) above and 4.251 m (167.375 in.) below the centerline of the outlet flange. The downcomer fluid was in full communication with fluid in the vessel at the lower extent of the downcomer. Meanwhile the downcomer/vessel flow path was completely blocked at the top of the downcomer (an axial elevation corresponding to the vessel head flange surface). The blowdown leg was connected to the vessel outlet flange. This leg consisted of a vessel outlet nozzle, an instrumentation test section, the break orifice, a shutoff gate valve, a rupture disk assembly, and a discharge pipe and tee. The 16 mm (0.6374 in.) break orifice was axially centered within the test section which was constructed of 0.3556 m (14 in.) Schedule 160 stainless pipe.

A measurement of the weight of the system throughout the blowdown was accomplished by four load cells which supported the entire weight of the system. These precision transducers, three of which supported the vessel, and one of which supported the blowdown leg were the primary means for determining the system weight. The mass flow rate through the orifice was indirectly determined by electronically differentiating the time-dependent weight of the system. This sytem had been tested and was determined from the engineering judgement of Wyle personnel to be accurate to within 0.5 kg/s of the actual mass flow rate at all times during the experiment. A six beam gamma densitometer, comprised of two three-beam densitometers mounted on opposite sides of the pipe, was used the determine the density of the exiting liquid/vapor mixture at three radial cross sections at a position 0.87 m (34.26 in.) upstream of the break orifice. The fluid temperature 0.87 m upstream of the break orifice and near the bottom of the vessel were measured by ISA Type K

thermocouples. The pressure 0.87 m upstream of the break orifice was measured by a pressure transducer.

The initial conditions for LOFT-Wyle test WSB03R were a system completely filled with demineralized water at pressure of 14.7MPa (2148 psia), a fluid temperature of 557K (542.9°F) at the bottom of the vessel, and a fluid temperature of 520K (476.3°F) measured 0.87 m upstream of the break orifice. Before initiating the blowdown, the system was allowed to 'soak' for three hours to equalize the temperature in the fluid and structural material. The blowdown through the 16 mm orifice was then initiated by venting a cavity between two 0.1524 m (6 in.) diameter rupture disks connected to the downstream flange of the blowdown line shutoff gate valve. As a result of a lack of detail in the description of this portion of the LOFT-Wyle facility, the rupture disks are estimated, from scaling of various facility sketches provided in Reference 1, to be 1.72 m (5.64 ft) downstream of the break orifice. The blowdown which begins with the venting and subsequent yielding of the rupture disks was simulated for 150 s.

Original Assessment Model

The input description for the original assessment is described in Volume III of the RELAP5/MOD2 Code Manual [2]. An electronic copy of the corresponding input deck was obtained from RELAP5-3D program developers, Idaho National Engineering and Environmental Laboratory (INEEL). In this model, the 5.4 m^3 (190 ft^3) pressure vessel, with downcomer in place was represented using 10 one-dimensional (1-D) volumes, 7 above the bottom of the downcomer and 3 below. The downcomer was modeled using 6 1-D volumes, 4 below the blowdown pipe, one at the elevation of the pipe, and one representing the flow skirt extension above the blowdown pipe. All junctions at which an area change occurred were modeled using the RELAP5 smooth area change option except for the two junctions connecting the upper portion of the vessel to the lower portion, and the lower portion of the vessel to the downcomer. Here the RELAP5 abrupt area change option was invoked. The blowdown pipe leading up to the break orifice was modeled using 4 horizontal 1-D volumes. The volumes representing the blowdown pipe were connected to the correct elevation of the downcomer using a cross flow junction. The 16 mm (0.6374 in.) diameter orifice itself was modeled using the RELAP5 abrupt area change option with an area equal to the actual orifice area. In the original model the default RELAP5 Ransom-Trapp critical flow model was used [4] with unity subcooled, two-phase, and superheated break flow multipliers. The blowdown line beyond the break orifice was not explicitly modeled. The attributes of the original assessment model are summarized in Table 1 under the heading Case 0.

Revised Assessment Model

In previous assessments of RELAP5-3D [5,6], it was concluded that faithful representations of the experimental facility including instrumentation, the boundary conditions and the initial conditions were required to obtain an undistorted assessment. This philosophy was used in the creation of the revised assessment model.

A slight error in the representation of the downcomer thickness in a previous assessment was found and corrected. As a result, the downcomer flow area was reduced 1.6% relative to the developmental assessment model. The RELAP5-3D fluid volume containing the instrumentation which records temperature, pressure, and fluid density upstream of the break orifice was also adjusted such that its cell-center corresponds to the location of the instruments. The initial vessel pressure was set to the correct experimentally measured value of 14.7Mpa (2148 psia). In addition, the initial sytem fluid temperatures were set to the experimentally measured values of 557K (542.9°F) in the vessel and 520K (476.3°F) upstream of the blowdown orifice.

The revised assessment model which initially was constructed from one-dimensional fluid components was also revised in several other areas. First, the experimental facility fluid components downstream of the 16 mm break orifice were modeled explicitly. These include the remainder of

blowdown spool piece #2, the shutoff gate valve, the rupture disk assembly, and the discharge piping from the rupture disks to the 'tee' outlet to the atmosphere. Secondly, the heat capacity associated with the structural material of the vessel downcomer and blowdown loop piping was modeled explicitly through the use of passive heat structures. In addition, in order to obtain better steady-state initial conditions for the transient blowdown calculation, the model was initialized for 10 seconds with the rupture disks intact.

In the new 1-D model the pressure vessel, with downcomer in place, was represented using 16 volumes, 14 above the bottom of the downcomer and 2 below. The downcomer was modeled using 11 volumes, 8 below the blowdown pipe, one at the elevation of the pipe, and two representing the flow skirt extension above the blowdown pipe. All junctions within the vessel and the downcomer regions were modeled as smooth. Form loss coefficients of zero were employed at all junctions except for those joining the lower vessel head to the downcomer and to the upper vessel regions. At these locations small form loss coefficients of 0.1 were employed, each representing one-half of those associated with a 180 degree piping bend. The blowdown pipe leading up to the break orifice (which includes spool piece #1 and the upstream portion of instrumented spool piece #2) was modeled using 6 horizontal volumes connected to one another with smooth junctions. The volumes representing the blowdown pipe were connected to the correct elevation of the downcomer using a side exiting junction with non-zero form loss coefficients calculated for the existing physical geometry (1.13 in the forward direction and 1.0 in reverse). The 16 mm (0.6374 in.) diameter orifice itself was modeled as a single abrupt junction with an area equal to the actual orifice area.

Volumetric fluid components downstream of the orifice included: 1) a single volume representing the first (smaller diameter) downstream portion of spool piece #2, 2) two volumes representing the final (larger diameter) downstream portion of spool piece #2, 3) two volumes to separately represent the inlet and outlet sections of the shutoff gate valve, 4) 8 volumes to represent the ~ 2.4 m long straight run of downstream piping, 5) a single volume which represents the 'tee' connected to the end of the downstream piping run, and 6) a time-dependent volume to represent atmospheric conditions beyond the 'tee'. All junctions between volumes downstream of the orifice were modeled as smooth, except for an abrupt area change at the rupture disk location (between the volume representing the downstream portion of the gate valve and the first volume representing the ~ 2.4 m long straight run of downstream piping). In addition, non-zero form loss coefficients were only applied to the junction representing the gate valve, the junction representing exit to the atmosphere, and the junctions at which an area change occurred. Passive heat structures were included in the revised model in order account for the heat storage capacity of the system vessel, downcomer, and blowdown piping run. The majority of the heat structures were modeled as cylindrical regions with best-estimate dimensions and compositions. In contrast, the partially hemispherical upper and lower regions of the vessel structure were modeled as two heat structure components, a slab and a cylindrical region. The thickness and surface area of these heat structures were adjusted to preserve the actual surface area and volume of the true vessel head structures. A schematic of the fluid component nodalization used in the revised 1-D LOFT-Wyle WSB03R test assessment model is presented in Figure 2.

Comparison of Model Results

In the initial revised assessment calculations both the default RELAP5 Ransom-Trapp [4] and optional Henry-Fauske [7] critical flow models were employed with unity break flow multipliers. In addition, the non-equilibrium parameter for the Henry-Fauske critical flow model was retained at its default value of 0.14. The attributes of these initial revised models are summarized in Table 1 under the respective headings, Case 1 and Case 2. As a consequence of high vapor velocities in explicitly-modeled test section components downstream of the orifice, Courant limitations caused the calculational time steps in the revised model to always be small. Thus, the calculational time step sizes were determined by the Courant limit and ranged from an initial value of 0.00156 s at the beginning of the transient gradually

increasing to a value of 0.0125 s at the conclusion of the transient.

Figures 3 through 6 compare three important fluid parameters obtained from these calculations (designated as Case 1 and Case 2) with those obtained experimentally and with those calculated with the original INEEL assessment model (designated as Case 0). These parameters include: 1) system pressure upstream of the break orifice, 2) break flowrate, 3) integrated break orifice mass flow, and 4) fluid density upstream of the break orifice. The experimental results for three of the four parameters include error bars. The error bars on the measured mass flow rate represent Wyle Laboratory's engineering judgement, while the error bars on pressure and density represent the stated uncertainty in the measurement equipment. The experimental value for integrated break orifice mass flow does not include error bars since this is an indirectly derived quantity.

Of the parameters being compared, the transient pressure measurement upstream of the orifice was judged to be the measured parameter with the least uncertainty. Figure 3 shows that the original assessment model overpredicts upstream pressure for the first ~950 seconds before falling in line with measurement at later times. The revised 1-D assessment model using the default Ransom-Trapp critical flow model slightly underpredicts pressure for the first 200 seconds of the transient while overpredicting pressure, sometimes significantly, from that time onward. This alternate prediction of pressure vice the original model is mainly the result of the addition of heat structures, which tend to keep pressure higher for a longer period of time by releasing stored heat energy into the fluid later in the transient. The inclusion of heat structures, which more faithfully represent the LOFT-Wyle experimental facility, bring to light fortuitous compensating errors in the time-dependent pressure calculated by the original assessment model. Meanwhile, the revised assessment model with the optional Henry-Fauske critical flow model also underpredicts pressure for the first ~250 seconds while subsequently overpredicting pressure from ~250 to 1000 seconds, beyond which time satisfactory agreement is acheived.

Figure 4 depicts the most significant parameter calculated by this experiment, the time-dependent rate of mass flow from the system. Here the original assessment model compares well with experimental data out to about 100 seconds, the high mass flow rate portion of the transient at which the fluid upstream of the orifice exists in a subcooled state. This good agreement is mostly fortuitous. This was proven to be a result of the incorrect initial fluid conditions in the original model through a sensitivity calculation run using the correct initial conditions in the original assessment model. From 100 seconds to ~400 seconds, the time period during which the level of the stratified two phase fluid upstream of the orifice is believed to remain above the centerline orifice position, the initial assessment underpredicts the mass flow rate. Beyond 400 seconds, where the level of the fluid upstream of the orifice is believed to fall below the orifice, the original model predicts the experimentally-observed drop in mass flow rate reasonably well. The revised 1-D model which uses the default Ransom-Trapp critical flow model, underpredicts the mass flow rate from the beginning of the transient out to ~400 seconds. Beyond this time the model overpredicts mass flow rate, especially the timing of the sharp drop in flow rate as the two-phase mixture drops below the level of the orifice. In the LOFT-Wyle experiment the break orifice is centered in the test spool piece oriented in the primary direction of fluid flow. In such case, if the horizontally-stratified water level is above or below the break orifice, the donered numerical scheme may underpredict or overpredict the junction void fraction. The horizontal stratification entrainment take-off model in RELAP5-3D [3] cannot be applied in this case since the orifice is not in an upward, downward, or side-centered orientation with respect to the upstream volume. Meanwhile, the revised assessment model using the Henry-Fauske critical flow model generally predicts the time-dependent mass flow rate from the system rather well, deviating from the experimental data somewhat at times less than 100 seconds and between 400 and 500 seconds.

Figure 5 depicts the time-integrated mass flow from the system. The curves shown in this figure are merely the integrals over time of the quantities

shown in Figure 4. Here the original assessment model compares rather well with experimental data except for a slight underprediction between ~100 and ~700 seconds, which corresponds to flow rate underprediction from ~100 to ~400 seconds and a compensating overprediction from ~400 to ~700 seconds. Meanwhile, the revised 1-D model which uses the default Ransom-Trapp critical flow model, significantly underpredicts integrated mass flow from the beginning of the transient out to ~700 seconds. Beyond this time the model overpredicts integrated mass flow, eventually exhausting a total of ~100 kg (220 lb) more fluid from the system by 1500 seconds than was observed experimentally. Finally, the revised assessment model using the Henry-Fauske critical flow model slightly underpredicts integrated mass flow from the beginning of the transient out to ~500 seconds. Beyond this time this model also overpredicts integrated mass flow, again exhausting a total of ~100 kg (220 lb) more fluid from the system by 1500 seconds than was observed experimentally.

The amount of fluid which was exhausted in the simulations is determined by the entrainment of liquid in the lower head of the vessel. The impact of interfacial drag on this phenomena will be discussed in a later section of this paper.

Figure 6 depicts the time-dependent average fluid density upstream of the orifice. Here the original assessment model mispredicts the timing of the large drop in fluid density which occurs at ~100 seconds, the subcooled to saturated transition point. This is again the result of incorrect initial fluid conditions. At ~500 seconds the original model does, however, predict the sharp drop in average fluid density due to the changing of fluid conditions upstream of the orifice from two-phase fluid to vapor rather well. The revised 1-D model which uses the default Ransom-Trapp critical flow model does a much better job of predicting the initial drop in fluid density at the subcooled to saturated transition point. However, the prediction of the drop in average fluid density during the two-phase to vapor transition occurs later than in the original assessment model, highlighting the fact that, in this case, more faithful facility modeling (i.e. inclusion of heat structures) uncovers fortuitous compensating errors in the time-dependent fluid density calculated by the original assessment model. Finally, the revised 1-D model which uses the Henry-Fauske critical flow model accurately predicts the initial drop in fluid density at the subcooled to saturated transition point. This model also predicts the timing of the drop in fluid density at ~500 seconds rather well. The fact that this model does not predict the experimentally measured density plateau between ~100 and ~400 seconds is most likely not a liability in the model, but is instead related to the manner in which this data was obtained. The reported experimental density is the average value from the three sets of densitometers. Since each densitometer only views a single chord cutting across the instrumentation spool, any given densitometer reading will exhibit a sharp density change as the two-phase mixture level falls through its narrowly-focused field of view. Since three densitometer readings (which pass through chords at different elevations) are combined to determine the average upstream mixture density, this average will tend to exhibit a sharply defined density change, rather than a gradual change as the level of the two-phase horizontally-stratified mixture level falls below the elevation of the highest densitometer beam.

Sensitivity to Choking Model Parameters

The orifice used in LOFT-Wyle test WSB03R is a unique design, with a length to diameter ratio of ~3.4. This orifice design does not directly correspond to any that was used to develop either the Ransom-Trapp or Henry-Fauske critical flow models. As such, input discharge coefficients for both models, as well as the 'non-equilibium' coefficient in the Henry-Fauske were 'tuned' to obtain better agreement with experimental data, primarily orifice mass flow or blowdown rate as a function of time. Figures 7 through 10 detail the best results obtained from this 'tuning' of the critical flow correlations in the break orifice of the revised assessment model. The attributes of these revised models with adjusted critical-flow parameters are summarized in Table 1 under the respective headings, Case 3 and Case 4.

Figure 7 shows that the revised 1-D assessment model using the Ransom-Trapp critical flow model with non-physical subcooled, two-phase, and superheated critical flow discharge coefficients of 1.2, still slightly underpredicts pressure for the first 200 seconds of the transient. However, from 200 to 800 seconds, while pressure is still overpredicted, the agreement with experiment is much improved over that obtained with unity Ransom-Trapp discharge coefficients in either the original or the revised LOFT-Wyle RELAP5 models. The use of critical flow discharge coefficients greater than 1.0 represents a non-physical situation, indicating that the Ransom-Trapp model is being used outside its range of applicability. This situation may be a common occurance, as alluded to in the section of the RELAP5-3D User's Guidelines which provides recommendations for break modeling [3]. Meanwhile, the revised assessment model was run using the Henry-Fauske critical flow model with a critial flow discharge coefficient of 0.84 and a non-equilibrium parameter of 1000, indicating a 'frozen' model, or one in which the velocities of the liquid and vapor through the orifice are assumed to be equal. This model yields the best overall prediction of the experimentally-measured pressure upstream of the orifice throughout the transient.

Figure 8 again depicts the time-dependent rate mass flow from the system. The revised 1-D model which uses the Ransom-Trapp critical flow model with critical flow discharge coefficients set to a non-physical value of 1.2 predicts the mass flow from the beginning of the transient out to ~400 seconds very well. Beyond this time the model still somewhat overpredicts mass flow rate. But, the time at which the mass flow falls sharply as the two-phase mixture drops below the level of the orifice is now much better predicted. Meanwhile, the revised assessment model using the Henry-Fauske critical flow model with a critial flow discharge coefficient of 0.84 and a non-equilibrium parameter of 1000, predicts the time-dependent mass flow rate from the system very well, including the timing of the drop in mass flow rate at ~400 seconds.

Figure 9 again depicts the time-integrated mass flow from the system (the time integration of the quantities shown in Figure 8). The revised 1-D model which uses the Ransom-Trapp critical flow model with critical flow discharge coefficients set to 1.2, somewhat underpredicts integrated mass flow from the beginning of the transient out to ~550 seconds. Beyond this time the model continues to overpredict integrated mass flow, exhausting a total of ~120 kg (264 lb) more fluid from the system by 1500 seconds than was observed experimentally. Meanwhile, the revised 1-D model using the Henry-Fauske critical flow model with a critial flow discharge coefficient of 0.84 and a non-equilibrium parameter of 1000 predicts integrated mass flow from the beginning of the transient out to ~450 seconds very well. Beyond this time this model also continues to overpredict integrated mass flow, exhausting a total of ~100 kg (220 lb) more fluid from the system by 1500 seconds than was observed experimentally.

Figure 10 depicts the time-dependent average fluid density upstream of the orifice. The revised 1-D model which uses the Ransom-Trapp critical flow model with critical flow discharge coefficients set to 1.2 does a good job of predicting the timing and magnitude of the drop in average fluid density when the two-phase mixture drops below the level of the orifice. Finally, the revised 1-D model which uses the Henry-Fauske critical flow model with a critial flow discharge coefficient of 0.84 and a non-equilibrium parameter of 1000, very accurately predicts the timing of the drop in fluid density at ~500 seconds. As stated previously, the fact that this model does not predict the experimentally measured density plateau between ~100 and ~400 seconds is most likely not a liability in the model, but an experimental measurement anomaly resulting from the use of a limited number of densitometers with a very narrow field of view.

Based upon the above observations from 1-D RELAP5-3D models it appears that the 'best' choice of orifice choking parameters for LOFT-Wyle blowdown test WSB03R are the Henry-Fauske correlation with a critial flow discharge coefficient of 0.84 and a non-equilibrium parameter of 1000 (e.g. Case 4).

One common observation can be made upon reviewing the revised 1-D RELAP5-3D results obtained with various choked-flow models (both with and without optimized discharge/non-equilibrium coefficients). That is, all revised calculations tend to overpredict the total fluid mass lost from the system over the course of the transient by ~100 kg. Based upon the results of previous studies [5] it is believed that this misprediction may be a direct consequence of a limitation in the ability of RELAP5-3D to accurately predict liquid droplet carryover in volumes with relatively high void fractions. This deficiency in calculating the magnitude of droplet carryover may be traced to inaccuracies in the prediction of drag between the liquid and vapor phases. RELAP5-3D uses the drift-flux velocity to determine the interfacial drag. The drift-flux velocity in turn depends on the flow regime. An indication of RELAP5-3D having difficulty predicting drift-flux velocity and thus interfacial drag in the LOFT-Wyle blowdown experiment may be obtained by observing Figure 11, the time-dependent liquid fraction at the junction between the lower vessel and the downcomer for calculational Case 4. Here large high-frequency oscillations are observed in the liquid fraction at the entrance to the downcomer. This is a direct consequence of the interdependencies inherent in the default Kataoka-Ishii drift-flux correlation [8] employed in RELAP5-3D. In this model the drift-flux velocity is dependent upon the flow regime which in turn is dependent upon the void fraction. Thus oscillations in the flow regime produce oscillations in the drift-flux velocity and interfacial drag which in turn cause the void fraction to oscillate, each inter-dependent component driving the next.

Interfacial Drag Study

In order to reduce these oscillations and, if possible, obtain a better prediction of the liquid carryover and thus the total fluid mass loss from the system during the transient, two optional drift-flux correlations were tested. These include: A) the Gardner correlation [9] (implemented with Card 1 option 82) with modified bubbly and slug flow regime interfacial heat transfer coefficients (Card 1 option 61) and B) the Vea-Lahey correlation [10]. The use of either of these drift-flux correlations requires the use of an alternate formulation for the drift-flux distribution parameter (Card 1 option 78). As discussed in detail in Reference 5, the Gardner drift-flux correlation, appropriate for large pipes (D>0.24 m), is independent of flow regime. But, its optional implementation in RELAP5-3D is dependent upon mass flux. The correlation is only used for low mass flux situations. For high mass flux situations the default Kataoka-Ishii drift-flux correlation is used. In addition, the modified bubbly and slug flow regime interfacial heat transfer coefficient (Card 1 option 61) used here in conjunction with the Gardner drift-flux correlation, uses a Laplace number formulation (independent of relative phase velocity) rather the default Weber number criterion to calculate bubble size. This formulation was shown to reduce oscillatory behavior in a previous analysis [5]. Finally, the Vea-Lahey drift-flux correlation, also appropriate for large pipes (D>0.2 m), is independent of both flow regime and mass flux.

Both the Gardner and Vea-Lahey drift-flux correlations were investigated separately in the 1-D RELAP5-3D model of the LOFT-Wyle WSB03R blowdown experiment with the Henry-Fauske critical flow model using a discharge coefficient of 0.84 and a non-equilibrium parameter of 1000 (frozen model). The attributes of these revised models with alternate drift-flux correlations are summarized in Table 1 under the respective headings, Case 5 and Case 6. The effect of these alternate drift-flux correlations on the time-dependent liquid fraction at the vessel/downcomer interface can be obtained by viewing the two curves on Figure 12. This figure shows that the Gardner drift-flux model (as implemented in RELAP5-3D) and associated modified bubbly and slug flow regime interfacial heat transfer coefficients dampen the calculated oscillation in the liquid fraction at the vessel/downcomer interface quite significantly after ~530 seconds into the blowdown. During time frame from ~500 to ~550 seconds liquid fraction oscillations persist, since RELAP5-3D uses the default Kataoka-Ishii drift-flux model at higher mass fluxes. In addition, Figure 12 shows that the Vea-Lahey drift-flux

model tends to predict distinct regions of oscillatory behavior, each ~50 to ~100 seconds apart, finally culminating in a continuous oscillation beyond ~1350 seconds. This behavior, although somewhat less oscillatory than that resulting from the use of the default Kataoka-Ishii drift-flux model, is not satisfactory.

In spite of the large effect on predicted liquid fraction at the vessel/downcomer interface, the use of the three alternative drift-flux models only have a small effect on comparison to measured test parameters. The most relevant product of this study of alternative drift-flux formulations is the effect on the total fluid mass lost from the system over the course of the transient. This effect is depicted in Figure 13. The Vea-Lahey drift-flux correlation calculates system fluid mass losses very similiar to those obtained with the default Kataoka-Ishii correlation (within 10 kg at all times). Meanwhile, one also notices that the Gardner drift-flux correlation slightly underpredicts (with respect to both experimental data and the Kataoka-Ishii correlation) the total fluid mass loss from the system out to ~500 seconds. After that point the Gardner correlation overpredicts system fluid mass loss. But, the overall agreement with the end-state experimental data has been improved. That is, the calculation employing the Gardner drift-flux model tend to overpredict the total fluid mass lost from the system over the course of the transient by only ~70 kg (155 lb) rather than ~100 kg (220 lb).

Three-Dimensional Modeling

At this time it was determined that the use of the new RELAP5-3D hydrodynamic modeling capability might further reduce the difference between the computational simulation and the LOFT-Wyle experimental results. This conclusion was based upon observations of the asymmetry of the experimental facility. The most significant asymmetry was the single blowdown leg containing the 16 mm (0.6374 in.) orifice connecting to only a small azimuthal sector of the downcomer.

In order to better model this experimental asymmetry, the eleven-volume downcomer region component as well as the two-volume lower vessel head component (as depicted in Figure 2) were converted from one- to three-dimensional fluid components. The conversion was performed in a straight-forward manner. The relatively thin 0.08731 m (3 7/16 in.) thick downcomer was modeled as cylindrical annulus with one radial node, 11 axial nodes (identical to the 1-D model), and 4 azimuthal nodes (each one a 90 degree sector). The lower vessel head component, which connects to both the downcomer and the central vessel region was also converted from a one-dimensional to a three-dimensional component. This component was modeled in cylindrical geometry with two radial mesh, with the outer ring of mesh set to be the same thickness as the downcomer. As was the case for the downcomer region, this 3-D component employed 4 azimuthal nodes, each a 90 degree sector. Axially this two-volume tall 3-D component employed the same heights as the original 1-D component. But, in order to model correctly the hemispherical lower vessel head (which rests entirely in the lower of the two axial volumes), the outer ring of volumes in the lower axial volume set was eliminated from the system by setting its junction connections to all other volumes to zero. In addition, the volumes of the four lower inner ring volumes were modified such as to maintain the true volume of the hemispherical lower vessel. Finally, the number of passive heat structures adjacent to either the downcomer or lower vessel head were multiplied by a factor of four, with a concurrent factor-of-four reduction in volume and surface area. The additional structures were necessary to accomodate the four azimuthal quadrants of the new three-dimensional fluid components. This heat structure representation ensured that the total structural mass and surface area would be equivalent in the three- and one-dimensional fluid component models of the LOFT-Wyle experimental facility.

Otherwise, the remainder of the RELAP5-3D model of LOFT-Wyle test WSB03R was not altered. This includes the use of smooth junctions with no form-loss coefficients (except for a small form loss of 0.1 which represents the 180 degree bend at the lower vessel/downcomer and lower vessel/upper vessel junctions) in the vessel/downcomer modeling. In addition, the

"best" critical flow model from the 1-D analysis was used in the system simulation employing 3-D fluid components. This model was the Henry-Fauske critical flow model with a discharge coefficient of 0.84 and a non-equilibrium parameter of 1000.

At first a preliminary RELAP5-3D calculation was run with the Gardner drift-flux model (with modified bubbly and slug flow regime interfacial heat transfer coefficients) to see if oscillations in the liquid fraction in any azimuthal quadrant of the vessel/downcomer interface persisted. Figure 14 shows that, unlike the case of the fully 1-D model, the Gardner drift-flux correlation does not reduce oscillations in the liquid fraction at the vessel/downcomer interface in the 3-D model. This calculation is designated as Case 7 in both the figure and in Table 1. Similar oscillations were obtained with both the default Kataoka-Ishii and optional Vea-Lahey drift-flux models. An option in RELAP5-3D known as the modified LeVeque momentum flux splitting option (Card 1 option 93) [13] was then activated in an attempt to dampen the oscillations in the liquid fraction at the 3-D vessel/downcomer interface. The calculation with these modeling attributes is designated as Case 8 in Table 1 and Figure 14.

As implemented in three-dimensional fluid components in RELAP5-3D, the LeVeque method permits varying proportions of the accurate but numerically unstable central-differencing scheme to be used in combination with the standard upwind differencing scheme. This technique is used to compute cell-centered fluid velocities from those directly calculated in adjacent junctions. The LeVeque method allows proportionately more central-differencing to be employed depending on how closely the spatially-varying velocity profile can be approximated as a linear function. In practice the LeVeque method produces more accurate results than the purely upwind differencing scheme, especially in situations where a stratified vapor/liquid interface is encountered. In addition, a modification of the LeVeque method allows the R-direction fluid momentum equations in cylindrical geometry to be solved much more accurately in volumes abutting the coordinate centerline. Both of the above-mentioned situations in which the modified LeVeque method should produce increased solution accuracy exist in the three-dimensional components of the LOFT-Wyle model.

The modified LeVeque method in conjunction with the Vea-Lahey drift-flux model was found to produce the least amount of oscillation in the liquid fraction at the vessel/downcomer interface. This general lessening of the oscillatory behavior is depicted in Figure 14. The modified LeVeque method was not found to be as effective in reducing liquid fraction oscillations if either the default Kataoka-Ishii or Gardner drift-flux models were employed.

Figures 15, 16, 17, and 18 compare, respectively, the time-dependent orifice upstream pressure, orifice mass flow rate, the time-integrated fluid mass lost from the system, and the orifice upstream density for the newly developed RELAP5-3D model of the LOFT-Wyle blowdown test with three-dimensional fluid components to that previously obtained using only one-dimensional components (e.g. Case 4 and Case 8 in Table 1). This 3-D model employed the Vea-Lahey drift-flux correlation, and the modified LeVeque momentum flux splitting option. Upon observation, these figures show that the salient calculation results are only marginally affected by: 1) the use of three-dimensional fluid components in the vessel and downcomer, 2) the use of the Vea-Lahey vice the default Kataoka-Ishii drift-flux correlation, or 3) the use of the modified LeVeque momentum flux splitting option. In addition, although not shown, the use of the two-phase stratified flow level tracking option in either the 1-D or 3-D fluid component RELAP5-3D models had no noticable effect on the pertinent results of either calculation.

The fact that the 1-D and 3-D results are so close was not expected, given the radially asymmetric connection of the blowdown leg to the downcomer in the experimental facility. These results do, however, confirm the proper operation of the multi-dimensional fluid component in RELAP5-3D. This was confirmed by detailed investigation of the RELAP5-3D output. A reasonable distribution of azimuthal fluid velocities was observed in the three-dimensional downcomer component. That

is, the azimuthal velocities were observed to be highest, azimuthally symmetric, and physically reasonable in comparison to blowdown leg velocities at the elevation of the blowdown leg. These azimuthal downcomer velocities were observed to retain symmetry but become progressively lower at other elevations.

It is believed that radial uniformity of the flow distribution at the entrance to the downcomer in the LOFT-Wyle blowdown experiment is the major reason why three-dimensional fluid modeling has little effect on calculated results.

Conclusions

The LOFT-Wyle test WS803R was used to perform an assessment of RELAP5-3D. Faithful representation of the experimental facility including instrumentation, the boundary conditions and the initial conditions is required in order to obtain an undistorted assessment. With this philosophy in mind, a new 1-D RELAP5 model of the LOFT-Wyle facility was created. The major differences/improvements between this model and the original 1-D RELAP5 assessment model were: 1) more accurate modeling of the dimensions of the downcomer, 2) more accurate modeling of the instrumentation locations upstream of the blowdown orifice, 3) more realistic modeling of experimental system initial fluid conditions, 4) modeling of the portion of the experimental facility beyond the break orifice, 5) the use of heat structures to model the heat capacity of the structural material immediately adjacent to the fluid, and 6) a larger number of fluid volumes in the representation of the experimental facility.

The net result of these model modifications/improvements is generally improved agreement with experimental measurement, with the RELAP5 default Ransom-Trapp critical flow model with unity discharge coefficients. Further improvements were observed if the optional Henry-Fauske critical flow model is employed, again with default values for the discharge and non-equilibrium coefficients.

Since the orifice being modeled has a length to diameter ratio of ~3.4 it is not well described as either a sharp or a long-tube break orifice. As a result, the independent parameters in both critical flow models were 'tuned' in order to achieve best comparison with experimental measurement, especially the time-dependent mass flow rate through the blowdown orifice. These 'tunable' parameters included, the subcooled, two-phase, and superheated discharge coefficients for the RELAP5-3D default Ransom-Trapp model and the discharge coefficient and non-equilibrium parameter for the optional Henry-Fauske critical flow model. Best results were obtained with the Ransom-Trapp model when all discharge coefficients were set to non-physical values of 1.2. Meanwhile, best results were obtained with the Henry-Fauske model when the discharge coefficient was set to 0.84 and the non-equilibrium parameter was set to 1000 (a 'frozen' model with equal liquid and vapor velocities in the orifice).

The overall best comparison with experimental data was obtained using the Henry-Fauske model with a discharge coefficient of 0.84 and a non-equilibrium parameter of 1000. But, the fact that all revised 1-D RELAP5-3D models overpredicted (by ~100 kg) the total fluid system mass loss during the transient remained a cause for concern. Based upon the results of previous studies [5] it is believed that this misprediction may be a direct consequence of a flaw in the ability of RELAP5-3D to accurately predict liquid droplet carryover in volumes with relatively high void fractions. This can be traced to inaccuracies in the prediction of interfacial drag, which in RELAP5-3D is a function of the flow-regime-dependent drift-flux velocity.

Upon further investigation, it was discovered that the 1-D RELAP5-3D model suffered from a severe oscillation in the liquid fraction at the vessel/downcomer interface beyond ~450 seconds into the transient. This behavior, very similar to that seen in a previous RELAP5-3D analysis [5], was determined to be a result of the flow regime dependence of the default Kataoka-Ishii calculated drift-flux velocity and the resulting interfacial drag. It was believed that by reducing these liquid fraction oscillations, a more accurate prediction of droplet carryover and thus time-integrated system fluid mass loss could be obtained. Towards this

end two other drift-flux velocity formulations, the Gardner and Vea-Lahey correlations, which are not flow regime dependent were tested. The Gardner correlation (with modified bubbly and slug flow regime interfacial heat transfer coefficients) was found to significantly reduce the oscillations in the liquid fraction at the vessel/downcomer interface. However, the elimination of liquid fraction oscillations only provided a slight improvement in the calculational prediction of total fluid system mass loss during the transient (an end-state overprediction of ~70 kg rather than ~100 kg).

In response to observed asymmetries in the experimental facility, the downcomer and lower vessel head regions of the RELAP5-3D model of LOFT-Wyle blowdown experiment were converted from one- to three-dimensional fluid components. However, in contrast to the fully one-dimensional model, which employed the Gardner drift-flux correlation, the Vea-Lahey drift-flux correlation in conjunction with the modified LeVeque momentum flux-splitting model were required to reduce liquid fraction oscillations at the vessel/downcomer interface in the 3-D model.

The basic level of agreement with experimental results remained unchanged with the introduction of three-dimensional fluid modeling. This insensitivity to more explicit flow modeling is most likely the result of the radial uniformity of the flow distribution at the entrance to the downcomer.

References

1. Lin, J.E., G.E. Gruen, and W.J. Quapp, "Critical Flow in Small Nozzles for Saturated and Subcooled Water at High Pressure," Basic Mechanisms in Two-Phase Flow and Heat Transfer Symposium at the Winter Meeting of the American Society of Mechanical Engineers, Chicago, Illinois, pp 9-17, 1980.
2. Ransom, V.H. et al., "RELAP5/MOD2 Code Manual, Volume III: Developmental Assessment Problems," EGG-TFM-7952, December 1987.
3. "RELAP5-3D Code Manuals, Volumes I, II, IV, and V," Idaho National Engineering and Environmental Laboratory, INEEL-EXT-98-00834, Revision 1.1b, 1999.
4. Trapp, J.A. and V.H.Ransom, "Calculational Criterion for Nonhomogeneous, Nonequilibrium Two-Phase Flows," *International Journal of Multiphase Flow*, pp 669-681, 1982.
5. Aumiller, D.L., E.T. Tomlinson, and W.G. Clarke, "A New Assessment of RELAP5-3D Using the General Electric Level Swell Problem," Presented at 2000 RELAP5 International Users Seminar, Jackson Hole, Wyoming, available as B-T-3320 from DOE Office of Scientific and Technical Information, 2000.
6. Tomlinson, E.T. and D.L. Aumiller, "An Assessment of RELAP5-3D Using the Edwards-O'Brien Blowdown Problem," Presented at 1999 RELAP5 International Users Seminar, Park City, Utah, available as B-T-3271 from DOE Office of Scientific and Technical Information, 1999.
7. Henry, R. E. and H.K. Fauske, "The Two-Phase Critical Flow of One-Component Mixtures in Nozzles, Orifices, and Short Tubes," *Journal of Heat Transfer*, **93**, pp 179-187, 1971.
8. Kataoka, I. and M. Ishii, "Drift Flux Model for Large Diameter Pipe and New Correlation of Pool Void Fraction," *International Journal of Heat and Mass Transfer*, **30**, pp 1927-1939, 1987.
9. Gardner, G., "Fractional Vapour Content of a Liquid Pool Through which Vapour is Bubbled," *International Journal of Multiphase Flow*, **6**, pp 399-419, 1980.
10. Vea, H.W. and R.T. Lahey, Jr., "An Exact Analytical Solution of Pool Swell Dynamics During Depressurization by the Method of Characteristics," *Nuclear Engineering and Design*, **45**, pp 101-116, 1978.
11. LeVeque, R.J., "Numerical Methods for Conservation Laws, Lectures in Mathematics," Birkhauser Verlag, Basel, 1992.

Table 1

Attributes of the Critical Flow and Interfacial Drag Models Used in This Assessment

Case	Critical Flow Model	Critical Flow Discharge Coefficient	Henry-Fauske Non-Equilibrium Parameter	Interfacial Drag Correlation	Momentum Splitting Option
0 (Original)	Ransom-Trapp	1.0	—	Kataoka-Ishii	Standard
Revised Fully 1-D Models					
1	Ransom-Trapp	1.0	—	Kataoka-Ishii	Standard
2	Henry-Fauske	1.0	0.14	Kataoka-Ishii	Standard
3	Ransom-Trapp	1.2	—	Kataoka-Ishii	Standard
4	Henry-Fauske	0.84	1000 (frozen)	Kataoka-Ishii	Standard
5	Henry-Fauske	0.84	1000 (frozen)	Vea-Lahey	Standard
6	Henry-Fauske	0.84	1000 (frozen)	Gardner-61	Standard
Revised Models with 3-D Lower Vessel and Downcomer					
7	Henry-Fauske	0.84	1000 (frozen)	Gardner-61	Standard
8	Henry-Fauske	0.84	1000 (frozen)	Vea-Lahey	LeVeque

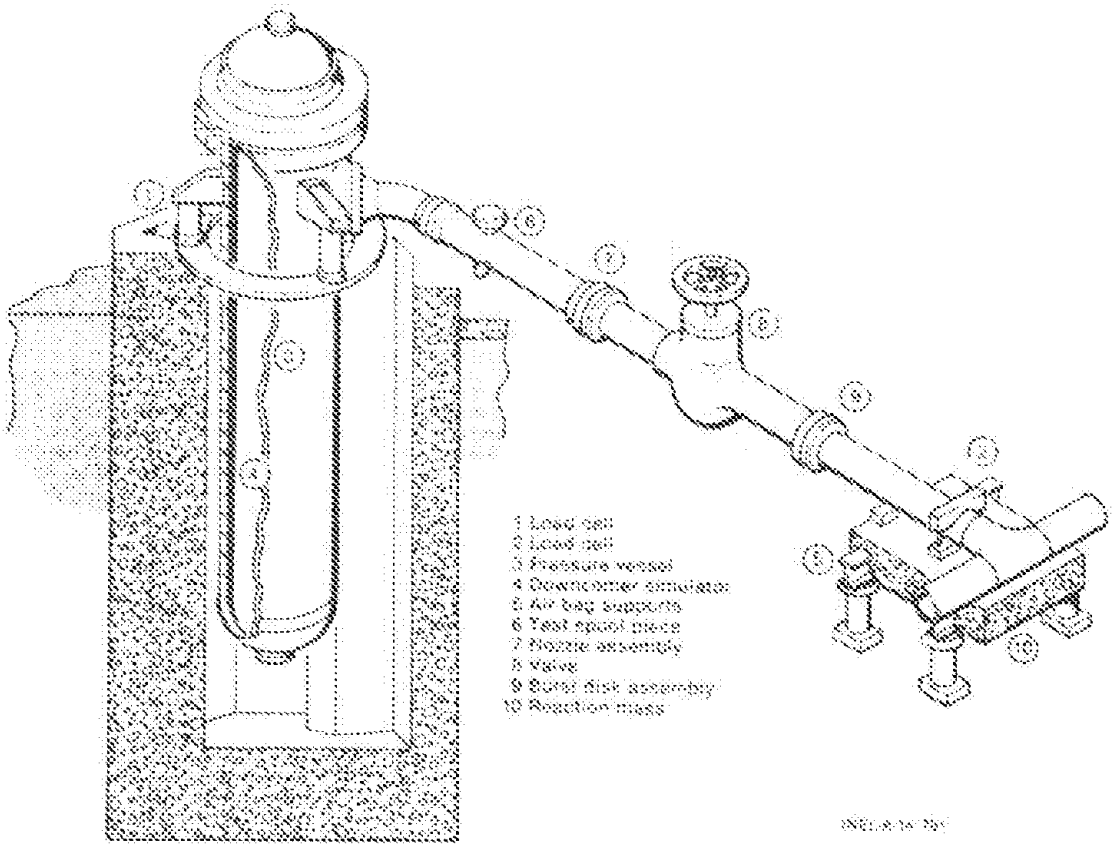


Figure 1
Axonmometric Projection of Wyle Test Facility

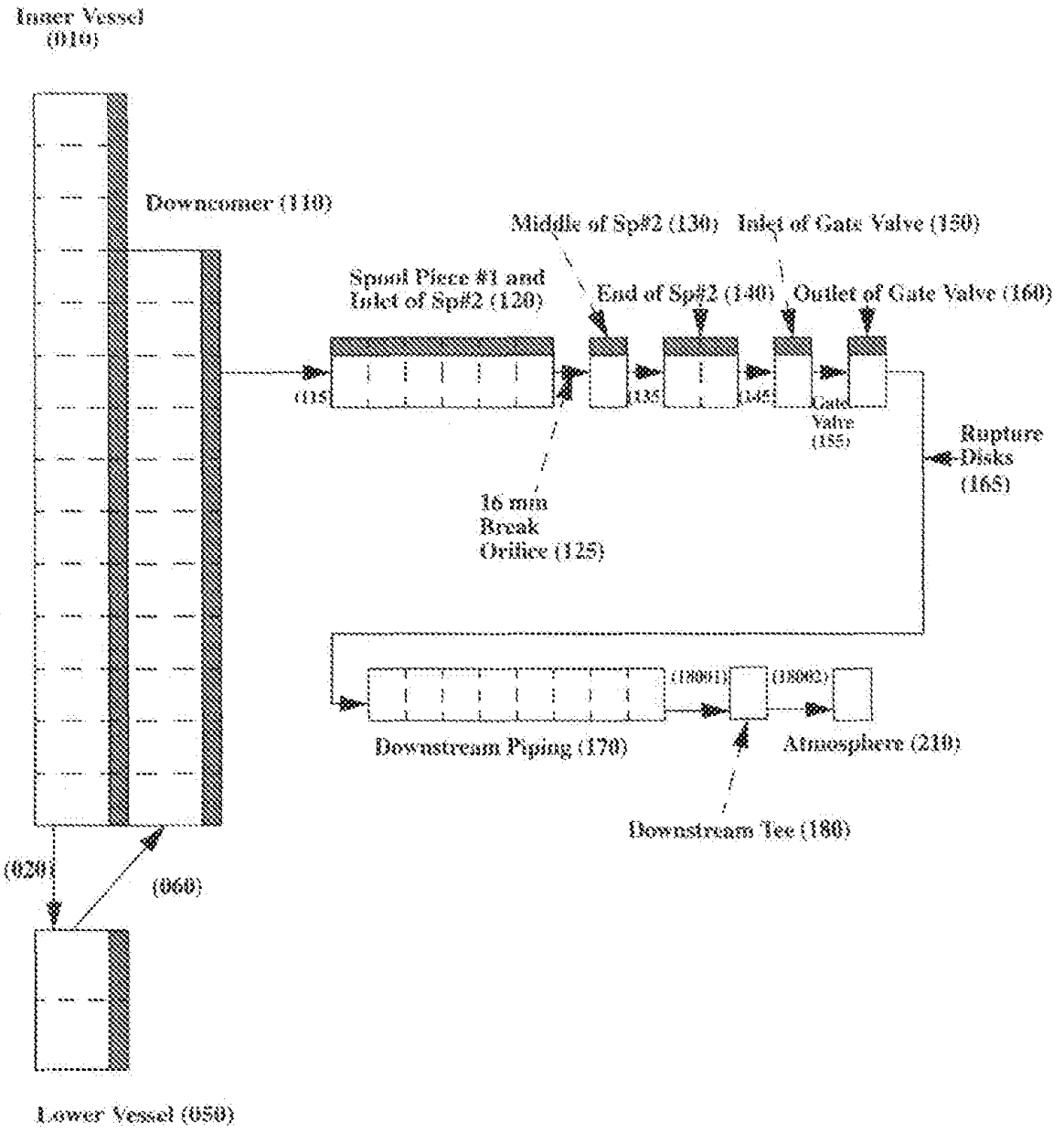


Figure 2
Schematic of RELAP5-3D Representation of LOFT-Wyle Experiment WSB03R

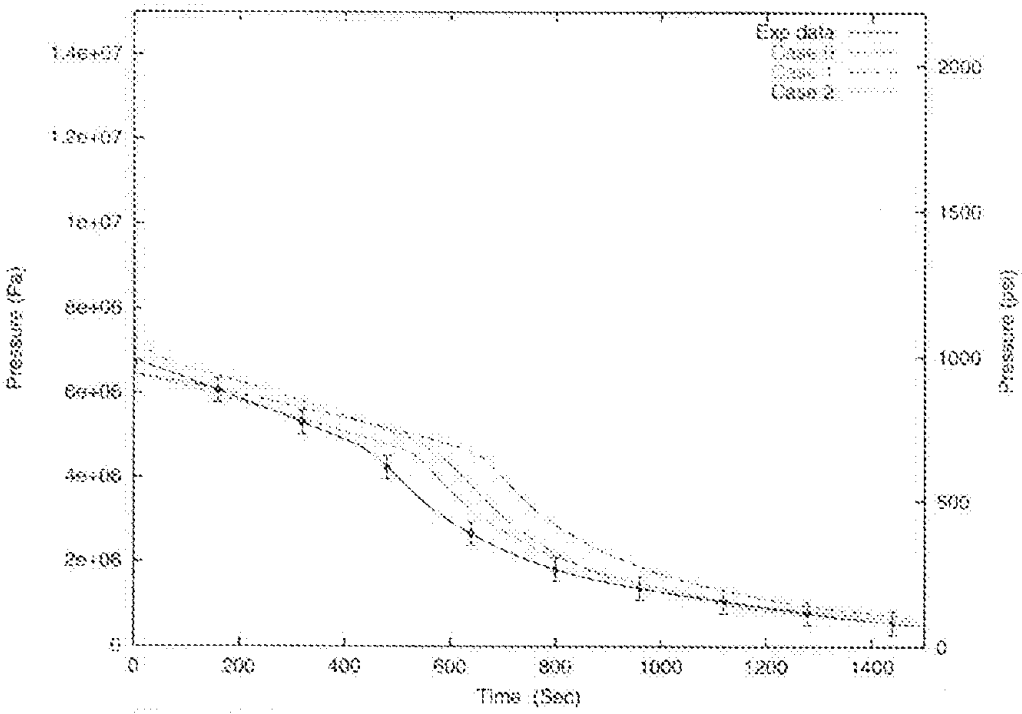


Figure 3: Initial Comparison of Pressure Upstream of the Orifice

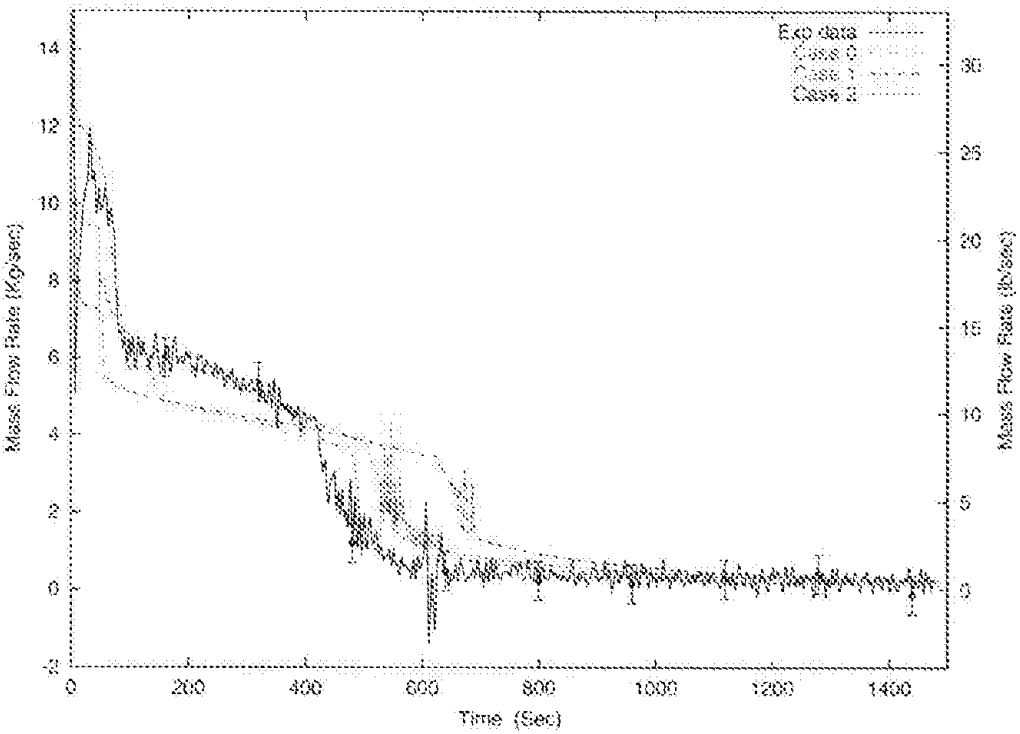


Figure 4: Initial Comparison of Rate of Mass Outflow

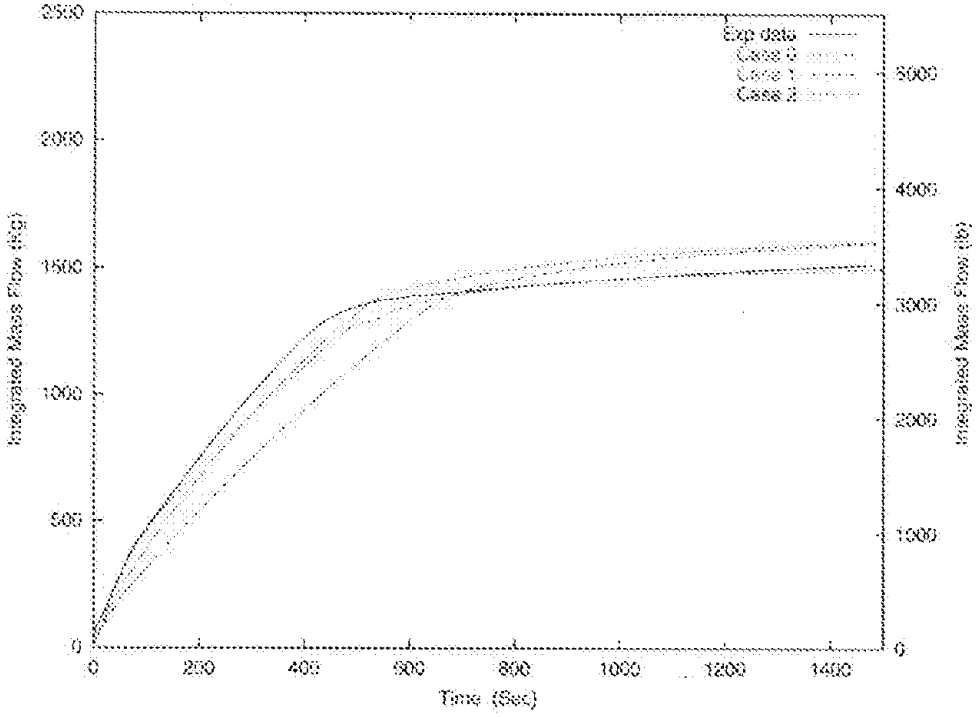


Figure 5: Initial Comparison of Integrated Mass Outflow

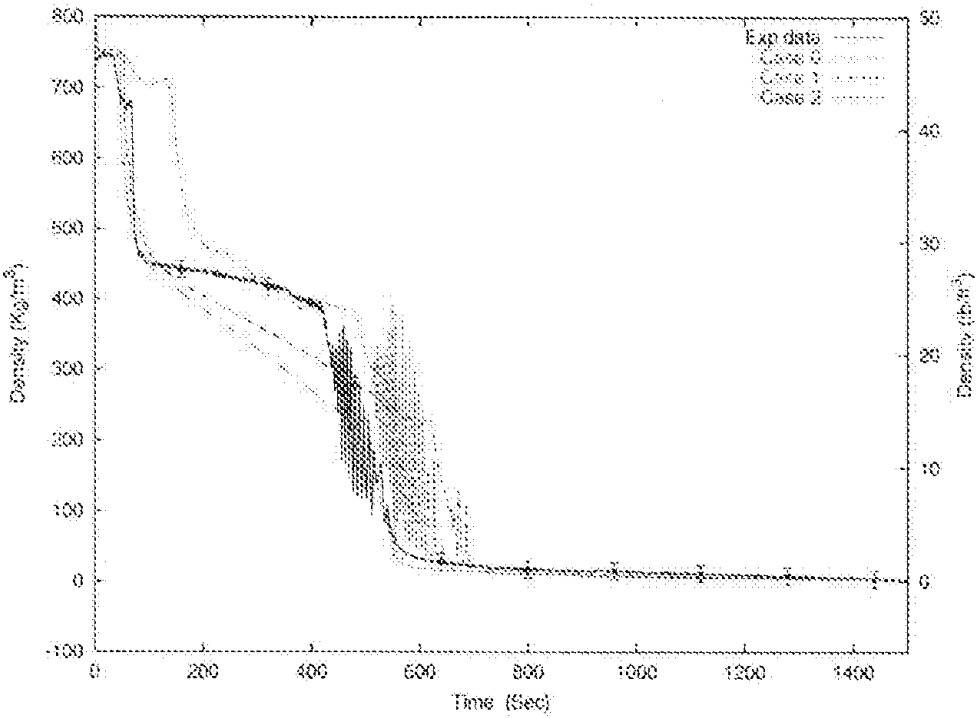


Figure 6: Initial Comparison of Density Upstream of the Orifice

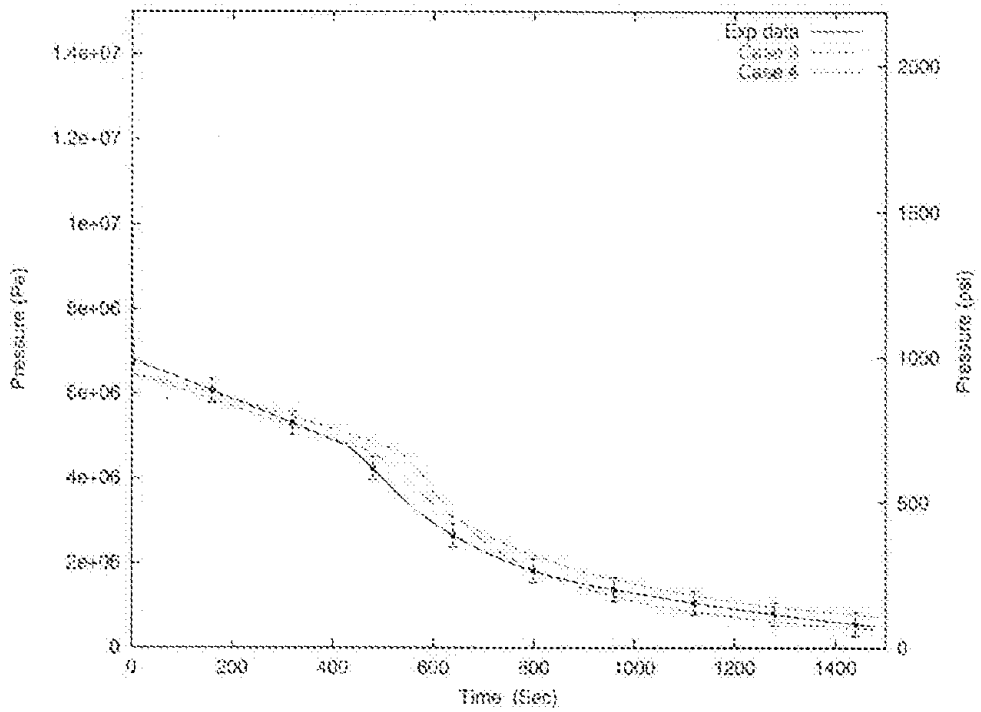


Figure 7: Comparison of Pressure Upstream of the Orifice Using Modified Discharge Coefficients

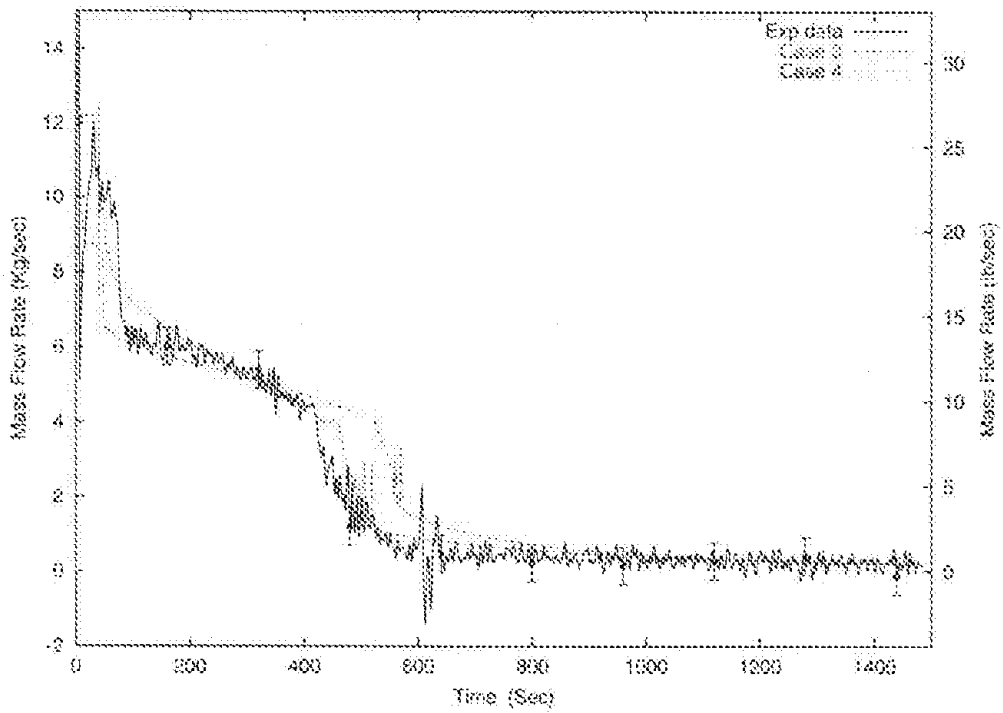


Figure 8: Comparison of Rate of Mass Outflow Using Modified Discharge Coefficients

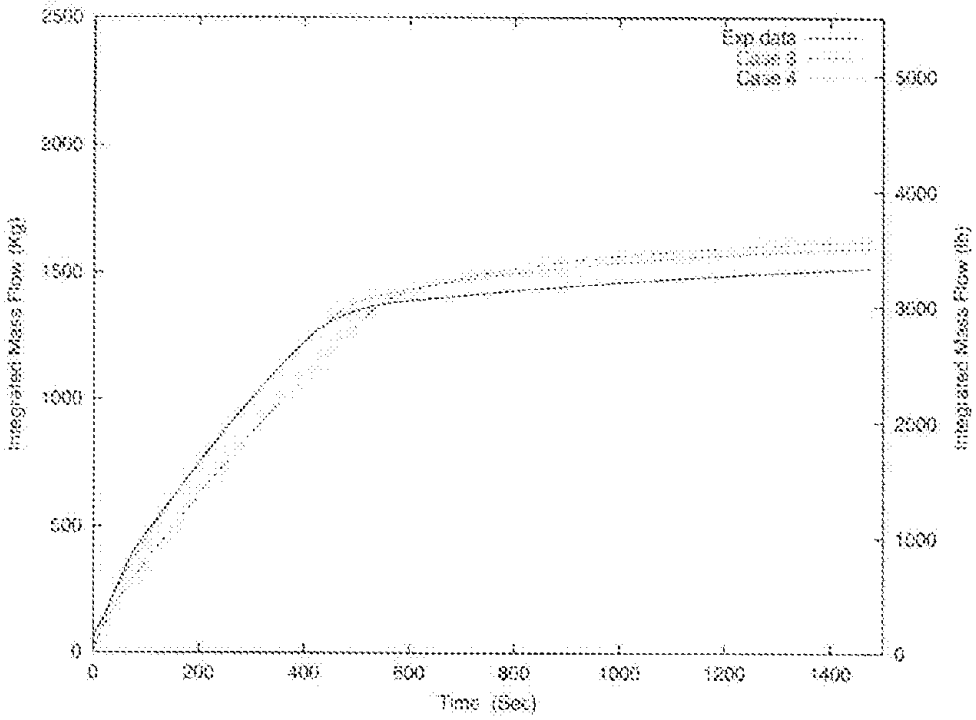


Figure 9: Comparison of Integrated Mass Outflow Using Modified Discharge Coefficients

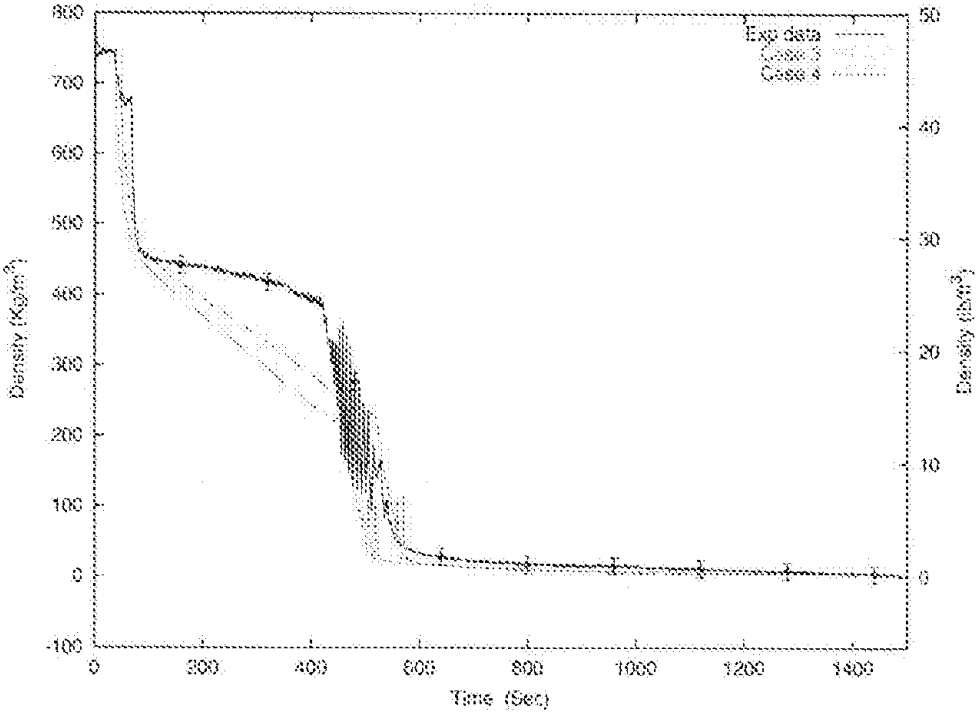


Figure 10: Comparison of Density Upstream of the Orifice Using Modified Discharge Coefficients

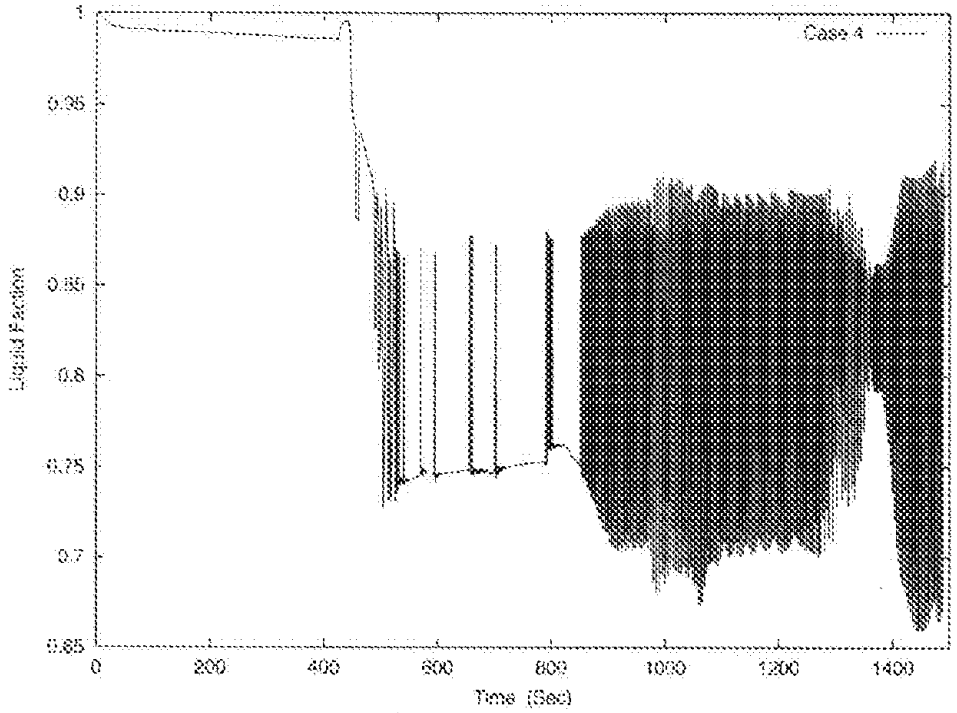


Figure 11: Liquid Fraction at the Vessel/Downcomer Interface

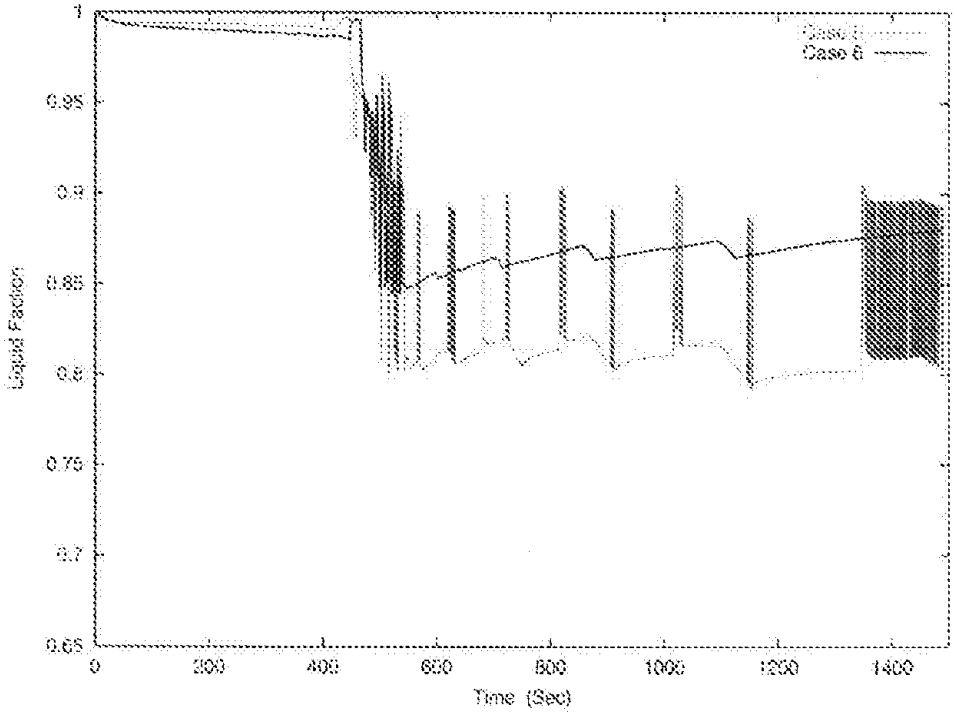


Figure 12: Liquid Fraction at the Vessel/Downcomer Interface Using Alternate Interfacial Drag Correlations

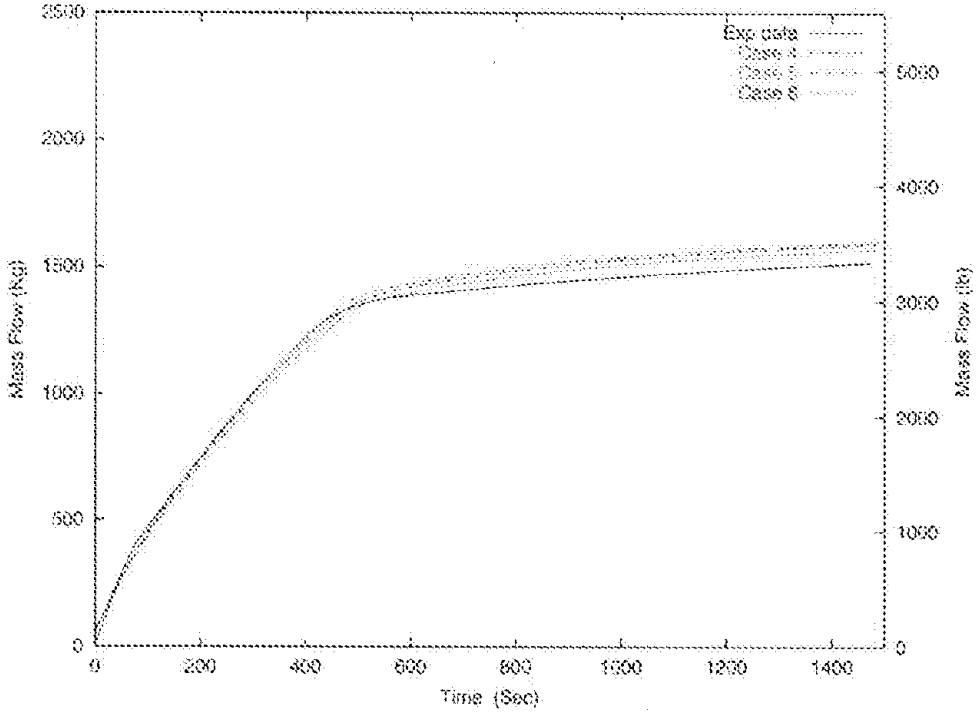


Figure 13: Comparison of Integrated Mass Outflow Using Various Interfacial Drag Correlations

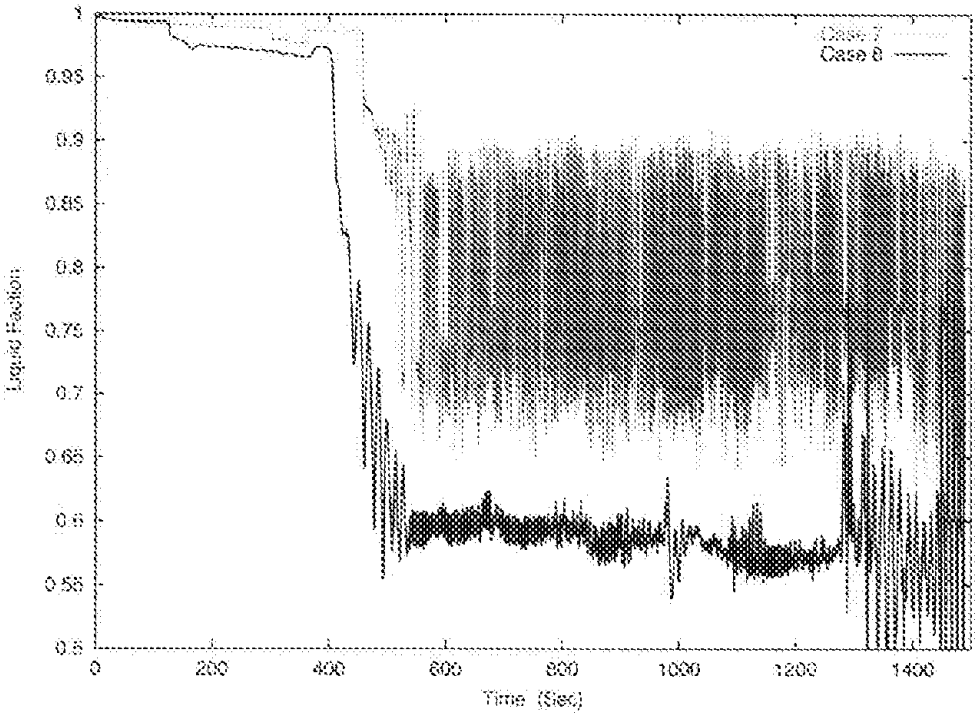


Figure 14: Liquid Fraction at the Vessel/Downcomer Interface in 3-D Calculations (same azimuthal quadrant as blowdown line)

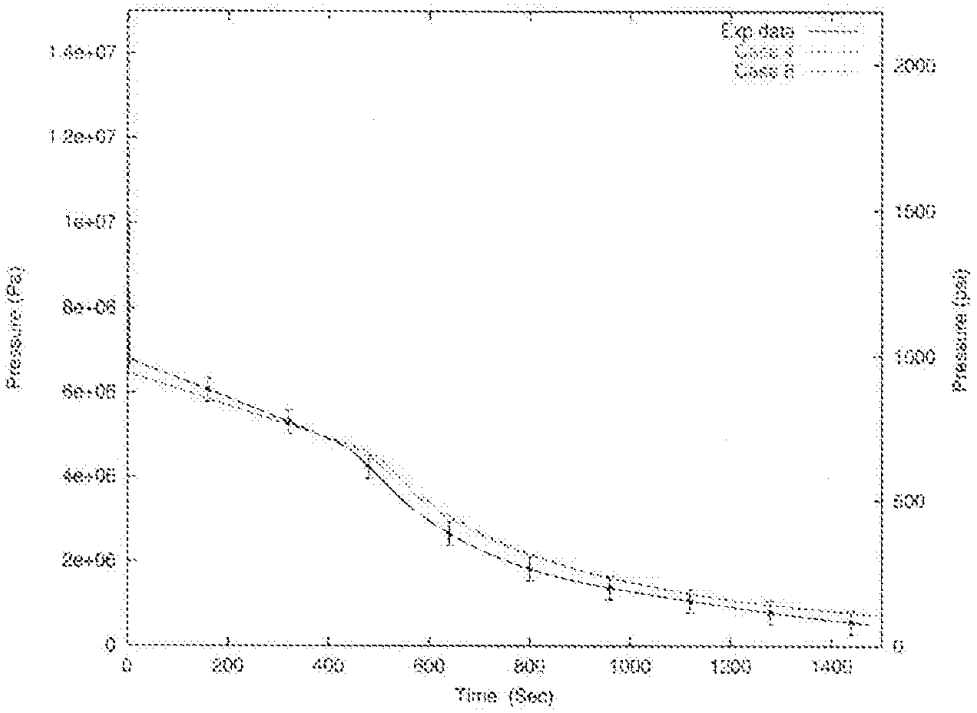


Figure 15: Comparison of Pressure Upstream of the Orifice (3-D Verses 1-D Modeling)

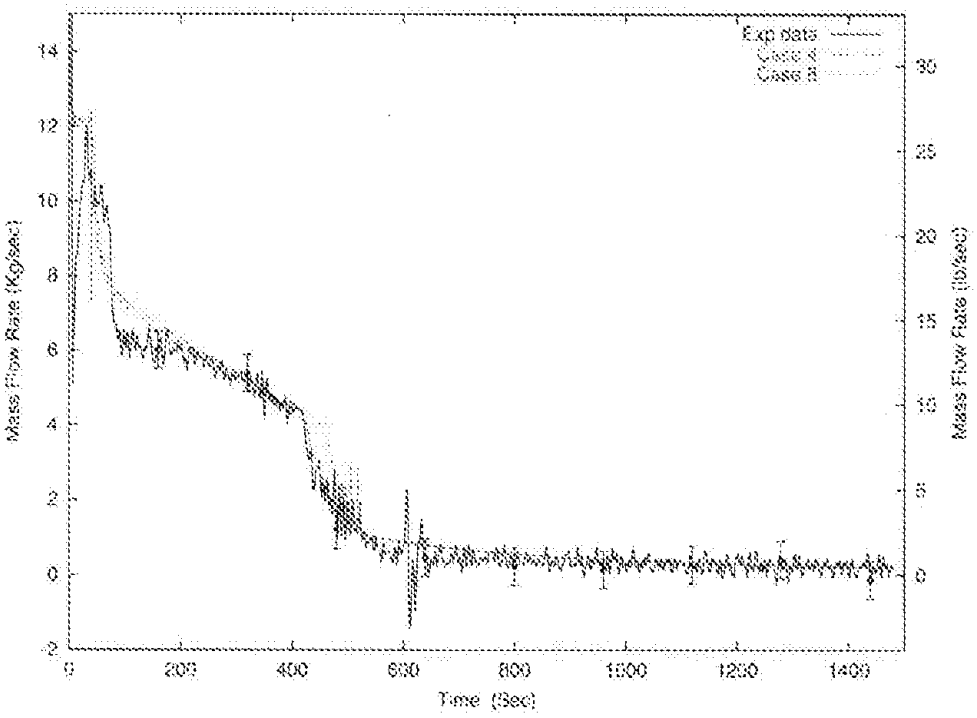


Figure 16: Comparison of Rate of Mass Outflow (3-D Verses 1-D Modeling)

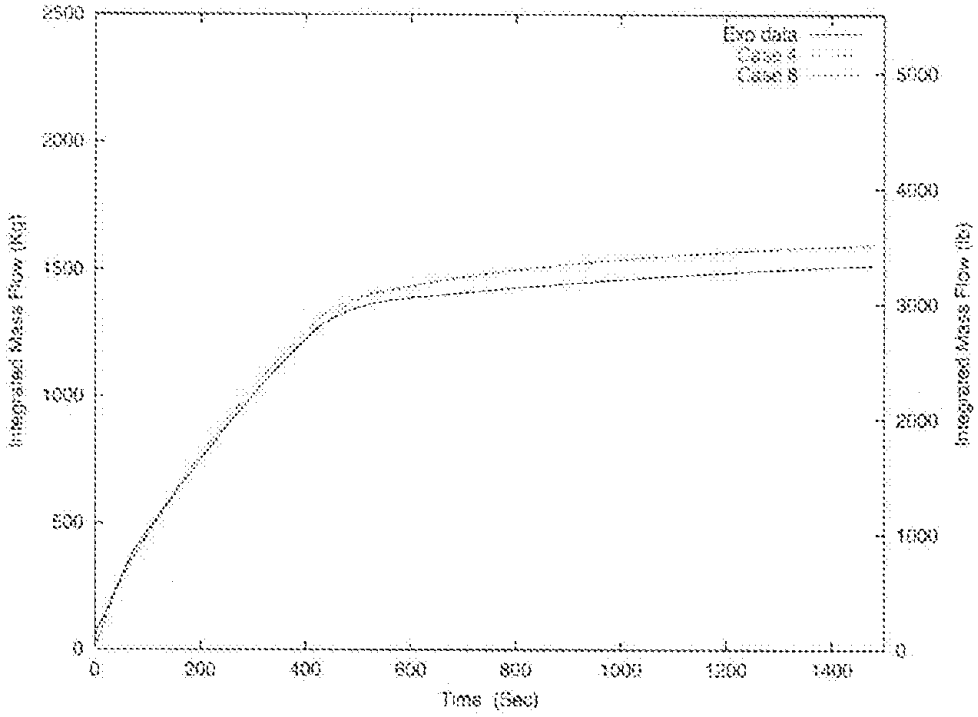


Figure 17: Comparison of Integrated Mass Outflow
(3-D Verses 1-D Modeling)

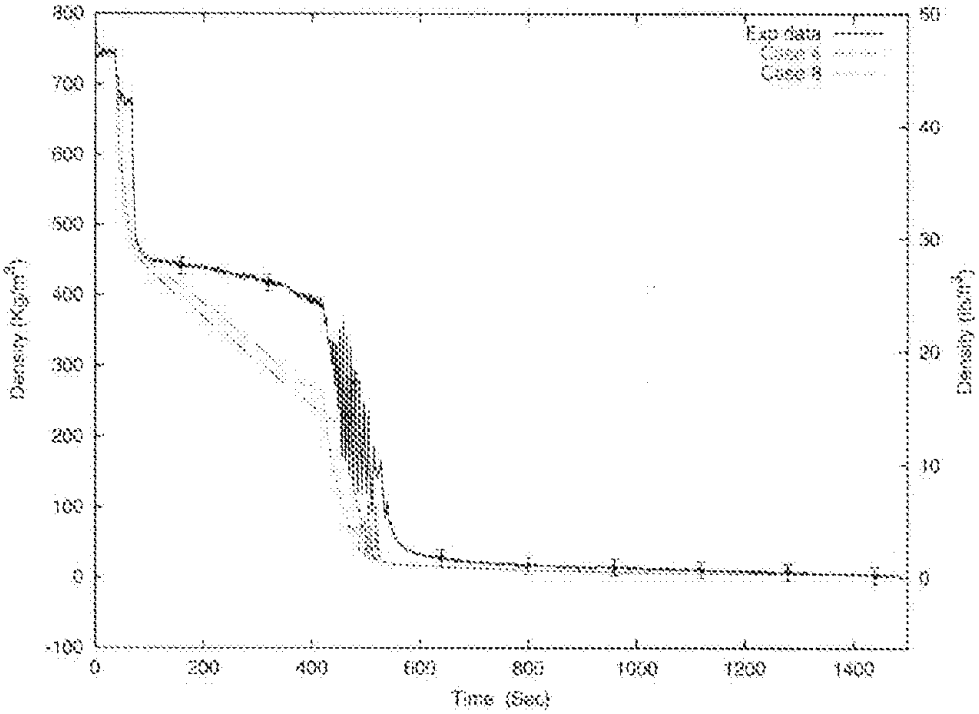


Figure 18: Comparison of Density Upstream of the Orifice
(3-D Verses 1-D Modeling)